Research Journal of Applied Sciences, Engineering and Technology 2(7): 642-653, 2010
ISSN: 2040-7467

Submitted Date: July 30, 2010 Accepted Date: August 20, 2010 Published Date: October 25, 2010

Numerical Simulation of Methane Triple Flames: Effect of Equivalence Ratio on the Flame's Structure

[1]A. Fossi, [1]M. Obounou, [1]D. Njomo and [1,2]R. Mouangue
[1]Department of Physics, Faculty of Sciences, LATEE, B.P 812 Yaoundé, Cameroon
[2]Department of Energetic Engineering, University Institute of Technology,
BP 455 NGaoundéré, Cameroon

Abstract: The present study offers a numerical investigation of the structure of triple flames formed in flow fields with a given equivalence ratio (ϕ = 1.8) in a two-dimensional duct flow configuration. We first use a mixture of methane and air at uniform temperature (T = 300 K) and velocity (0.3 m/s) at the inlet of the duct. The validation of numerical result is done by comparing with the experimental measurements of I.K. Puri, S.K. Aggarwal, S. Ratti and R. Azzoni. Second, detailed structure and chemical reactivity information are presented for four different equivalence ratios in order to determine its impact on flame structure. Triple flames consist of three reaction zones which merge at « triple point » and may be produced in stratified mixtures undergoing combustion. They may play some important roles in the stabilization and liftoff of laminar non premixed flames, in the building of new combustion models and in the mechanism of NOx reduction.

Key words: Laminar flow, numerical simulation, partial premixed combustion, premixed combustion, triple flames

INTRODUCTION

Triple flames, also called tribranchial consist of two premixed reaction zones (one fuel-rich and the other fuel-lean) and a nonpremixed reaction zone. They belong to the more general class of Partial Premixed Flames (PPFs). The two premixed reaction zones form the exterior "wings" of the flame while the non premixed reaction zone form the non premixed flame (as the result of an excess fuel and oxidizer from respective rich and lean premixed reaction zone mixed in stoichiometric proportion), is enclosed in between these two wings. Triple flames occur in most part of practical configurations namely when there are incomplete mixing of fuel and air, eg lean-burn gas-turbine engines (Owston and Abraham, 2010). Triple flames have some important applications: they are used in the stabilization and liftoff of laminar nonpremixed flames, in the building of new combustion models and in the mechanism of NOx reduction (Onuma *et al.*, 2001). Therefore, the structure of triple flames needs to be adequately investigated. There are excellent theoretical, numerical and experimental investigations of flames and particularly that of triple flames (Phillips, 1965; Dold, 1989; Kioni *et al.*, 1993; Muniz and Mungal, 1997; Ruetsch *et al.*, 1995; Schefer and Goix, 1998; Puri *et al.*, 2001; Noda and Yamamoto, 2006; Obounou *et al.*, 1994). From these sources and others, some propagation behaviors and structural characteristics of triple flames are known.

Triple flames were first reported by Phillips (1965) who investigated their propagation in a methane mixing layer in a horizontal configuration. He was particularly interested in determining the flame speed and the volume in the context of explosive conditions that occur at the roof of coal mine roadmaps. Thereafter, Dold (1989) performed a theoretical investigation on the propagation speed of the triple flame in the presence of a slowly varying mixture fraction gradient. He discovered that the flame speed increases as the mixture fraction gradient decreases, and it is bounded by the maximum adiabatic laminar flame speed of the system.

Phillips (1965) found the variation of the flame speed with the mixture fraction gradient to be consistent with the predictions made by Dold (1989). He suggested that the flame speed is higher for low mixture fraction gradients because the flame is flatter and the preheating of the unburned mixture is more efficient under these conditions. However the absolute flame speeds were higher than the adiabatic speed of corresponding stoichiometric premixed flame. Kioni *et al.* (1993) obtained a similar result by defining the flame speed as the mean flow velocity at the location of the flame. They have reported on an experimental investigation of a lifted triple flame stabilized in a coflowing stream. They observed that the width of the premixed "wings" increases as the mixture fraction gradient decreases. In addition the velocity profile at the leading edge of a triple flame was examined as a function of the transverse mixture fraction gradient.

Muniz and Mungal (1997) experimentally investigated the velocity profile at the base of a lifted jet flame and found it to be similar to the prediction of

Corresponding Author: M. Obounou, Department of Physics, Faculty of Sciences, LATEE, B.P 812 Yaoundé, Cameroon

Ruetsch *et al.* (1995). In particular they observed that the flame stabilizes itself in the region where the velocity is closed to the premixed laminar flame speed. Schefer and Goix (1998), extended the work of Muniz and Mungal (1997) regarding the applicability of laminar triple flame concepts to the stabilization of lifted turbulent jet flames, and concluded that this is not straight forward, since turbulence caused distortions in the velocity field.

Studies of the structure of triple flames have been undertaken for various fuels and setups. But studies using methane are most prevalent. This interest is due to the ability of the fuel to be produced from renewable resources and the fact that the methane is a major component of natural gas.

The objective of the current work is to perform a numerical investigation of the methane triple flames' structure by using a CFD package FLUENT (FLUENT, 6.3.26) modified such as to deal with Westbrook's formula of reaction rate (Westbrook and Dryer, 1981). By the present work, we intend to contribute to the understanding of the triple flame's structure. The process of generation of the triple flame is illustrated in Fig. 1 and consists of two premixed combustion (lean and rich). We first validate our numerical approach by comparison with experimental measures of Puri *et al.* (2001) and finally, we determine the effect of the increase of equivalence ratios on flames' structure.

MATERIALS AND METHODS

Numerical configuration and calculation conditions: We numerically investigated laminar triple flames formed in flow fields with a particular value of the equivalence ratios in a two-dimensional duct configuration expanded downstream to stabilize the flames, as depicted schematically in Fig. 1. This configuration was originally developed by Puri *et al.* (2001) in their experimental investigation. The fuel is methane, the oxidizer is air. In the duct, we burn simultaneously from both side of the inlet of the duct, a lean and rich mixture of methane and air (15.5 and 3.75 mm, respectively). The temperature and velocity are uniform. The boundary conditions uses in our calculations are presented in Table 1. The same conditions have been used by Puri *et al.* (2001) in their experiment.

Formulation: We consider flow with low Mach-number. Some others assumptions were employed in order to study our steady triple flames:

- The methane is assumed to be an ideal gas,
- The Lewis number is unity,
- The reaction of methane and oxygen obeys a single-step, irreversible Arrhenius law,
- The Soret and Dufour effects and the pressure gradient diffusion are negligible,

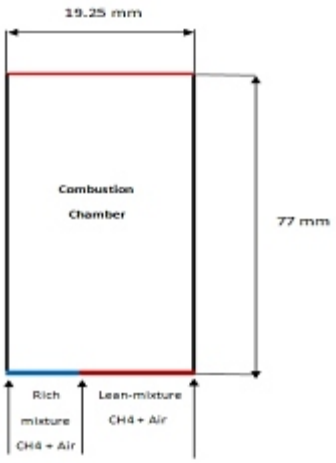

Fig. 1: Combustion chamber with different inlets

Table 1: Boundary conditions at the inlet of the duct

T (K)	U_0(m/s)	ϕ_{in}	ϕ_{out}	$\phi_{overall}$
300	0.3	1.8	0.35	0.6

- The thermal radiation and the bulk viscosity are negligible
- The viscosity and the pressure fluctuation terms in the energy equation are negligible.

On the bases of these hypothesis the governing equations that we solve is given by:
The continuity equation

$$\frac{\partial \rho U_j}{\partial x_j} = 0 \quad (1)$$

the momentum equation

$$\frac{\partial (\rho U_i U_j}{\partial x_j} = -\frac{\partial P}{\partial x_i} + \frac{\partial \tau_{ij}}{\partial x_j} + \rho g_i \quad (2)$$

here,

$$\tau_{ij} = \left(\lambda \frac{\partial U_i}{\partial x_i}\right)\delta_{ij} + \mu\left(\frac{\partial U_i}{\partial x_j} + \frac{\partial U_j}{\partial x_i}\right) \quad i = 1, 2$$

the species-masse equation

$$\frac{\partial (\rho U_i Y_k)}{\partial x_i} = \frac{\partial J_i^k}{\partial x_i} + \rho \omega_K \quad (3)$$

k = 1, 2,…, 5
and the energy equation

$$\frac{\partial (\rho U_i h_T)}{\partial x_i} = \frac{\partial}{\partial x_i}(J_i^E + U_j \tau_{ij}) \quad (4)$$

Here $J_i^k = \rho D \frac{\partial Y_k}{\partial x_i}$ and $J_i^E = \frac{\lambda}{C_P}\frac{\partial h}{\partial x_i}$ with $\rho D = \lambda / C_{pm}$ Closure of the system of equation (1)-(4) is achieved through the ideal-gas equation of state

$$\frac{P}{\rho} = RT\sum_{k=1}^{N}\left(\frac{Y_k}{W_k}\right)$$

Moreover the mixture enthalpy h is related to temperature by its definition in terms of the species enthalpy namely:

$$h = \sum_{k=1}^{N} Y_k h_K \text{ with } h_k = \int_{T_0}^{T} Cpk dT + \Delta H_k^0$$

The source term in equation (4) is given by $\omega_k = (\nu_k'' - \nu_k')W_k\omega_k$. In the present work, we evaluate each according to the reaction rate of methane formulated by Westbrook and Dryer (1981):

$$W_{CH_4} = -AT^n \exp(-E/R_0T)(\rho Y_{CH_4}/W_{CH_4})^a(\rho Yo_2/Wo_2)^b$$

where, n = 0, a = -0.3, b = 1.3, A = 1.3×10^8 $_S$ and E = 48.4 Kcal/mol.

As $$\phi = \frac{\left[Y_{CH_4}/Yo_2\right]}{\left[Y_{CH_4}/Yo_2\right]_{st}}$$

we deduce:

$$Y_{CH_4} = \frac{\phi\left[Y_{CH_4}/Yo_2\right]st}{\phi\left[Y_{CH_4}/Yo_2\right]st + 4.29}$$

and

$$Yo_2 = \frac{1}{4.29}\left(1 - \frac{\phi\left[Y_{CH_4}/Yo_2\right]_{st}}{\phi\left[Y_{CH_4}/Yo_2\right]_{st} + 4.29}\right)$$

Numerical method:

Combustion model: The governing equations are solved using the CFD package FLUENT (FLUENT User Manual, 6.3.26; FLUENT UDF User Manual, 6.3.26) modified with User Defined Functions in order to integrate the reaction rate formula proposed by Westbrook and Dryer (1981). We have used the finite rate approach. The solver is the steady segregated used with the implicit formulation. The Under relaxation factors for pressure, density, body forces, species and energy are presented in Table 2. We have applied the first-order up-wind scheme to each term of the transport equation.

Table 2: Under-relaxation factors

P	Density	Body forces	Momentum	Yi	Energy
0.3	1	1	0.7	0.9	0.4

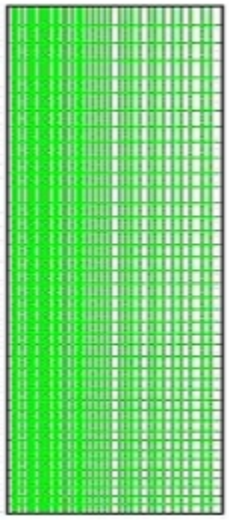

Fig. 2: Mesh of combustion chamber

Meshing: The computational space is divided by a staggered non uniform quadrilateral cell. The dimensions of the computational domain are 19.25 mm in the lateral direction (x) and 77 mm in the streamwise direction (y). The system is represented by a mesh system of (x×y) = (176×262 = 46112) as presented in Fig. 2. The reaction is initiated by using a burnt gas at high temperature (T = 1800 K).

RESULTS AND DISCUSSION

We intend to contribute to the understanding of the triple flames' structure. Therefore it is necessary to validate our simulation method by choosing a particular case (with parameters presented in Table 1).

Global flame structure: We present the contour temperature and reaction rate in Fig. 3 and 4, respectively.

From the contour of temperature presented in Fig. 4, we can reported a good agreement with experiment in terms of flame liftoff and the maximum temperature (temperature at "triple point" that is 2195 K for experiment and 2230 K for prediction). We present in Fig. 5 the profile of temperature at different positions in streamwise direction for four different positions (y = 5, 10, 15 and 18 mm). The temperature increases gradually between 0 and 8 mm, this region corresponds to the global

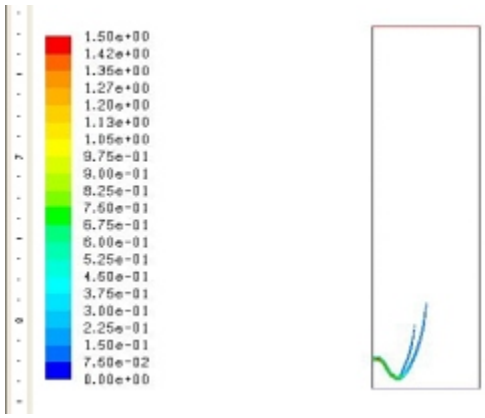

Fig. 3: Contour of reaction rate (in unit of mol/m^3/s)

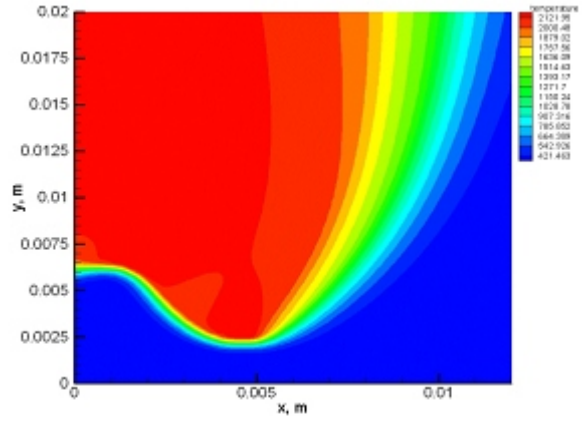

Fig. 4: Contour of temperature (in unit of K)

reaction zone, but there are some differences which may be related to the chemical kinetic scheme employed in the reaction rate formula. In fact, in the combustion model, we have used the Arrhenius formulation of reaction rate without dependence on temperature. Temperature dependence rate of reaction may directly relate the regions of maximum temperature with that of high chemical activity and consequently give a better prediction of temperature.

In order to validate the computational code, we present in Fig. 6, 7, 8 and 9 the profiles of species in the streamwise direction at different transverse displacements of the flame discussed in context of Fig. 3 and 4.

Measured and predicted streamwise species fraction mass profiles for the burner-stabilized flame are presented for three transverse displacements (namely x = 0, 6 and 10 mm), respectively for reactants (CH_4 and O_2) and products (CO_2 and H_2O) which are always the most abundant species in different methane-mechanisms.

Figure 6 shows streamwise species concentration of methane for the flame. There is a reasonable agreement between measurements and predictions along x = 0, but just a qualitative agreement for the remainder. In fact the transverse displacement x = 6 mm and x = 10 mm is situated in the lean side where the diffusion process for methane is more present. In Fig. 7, we observe a similar result, that is good agreement for x = 6 mm and x = 10 mm and just a qualitative result for x = 0 as the diffusion of oxygen at this position is more present. Reactants (CH_4 and O_2) are consumed in the global reaction zone while product (CO_2 and H_2O) are formed.

Figures 8 and 9 present the mass fraction of product (CO_2 and H_2O) we observe a good agreement with some results and considerable difference between measurements and predictions for others. We globally under-estimate product in our computational results, this fact may be related to the reaction rate formulation as shown by Obounou *et al*. (1994) in their work relative to detail chemistry in combustion model.

Figure 2 presents the contour of reaction rate, we can observe the different wings of triple flame (lean premixed flame, rich premixed flame and non premixed flame) which merge at "triple point", and finally we can report the liftoff of our triple flame. Figure 10 presents the profile of reaction rate for different positions above the burner in streamwise direction y = 3, 5, 7 and 10 mm. It is seen that for y = 3 mm, there is just a single maximum of reaction rate indicating the position of the triple point. For increasing values of y, the reaction rate present two maxima, each maximum indicating one of the premixed flames; the minimum value between the two maxima represents the reaction rate in the non premixed flame. We deduce that the three "wings" of triple flame are obtained for particular positions in streamwise direction (after the triple point position). The reaction zone topography in the steady laminar flame as presented in Fig. 2 enables us to distinguish the outer lean premixed zone, the inner rich premixed reaction zone and the non premixed reaction zone (result of the burning of oxidized fuel and oxidizer in stoichiometric proportion, where the oxidized fuel and oxidizer come from rich and lean premixed reaction zones, respectively).

4- 2 Effect of the inner equivalence ratios on triple flames structure: As the Equivalence ratios is directly related to the mass fraction of fuel and oxidizer trough the relation mentioned above, we propose to study the effect of its increase on the triple flames' structure. For this reason, we consider four different values and maintain the previous boundary conditions for the remainder parameters as shown in Table 3.

The above contours of temperature (Fig. 11) enable us to deduce the decrease of maximum temperature with the increase of inner equivalence ratio (mass fraction of fuel in rich mixture). We can explain it by the fact that for small inner equivalence ratio, we are around the

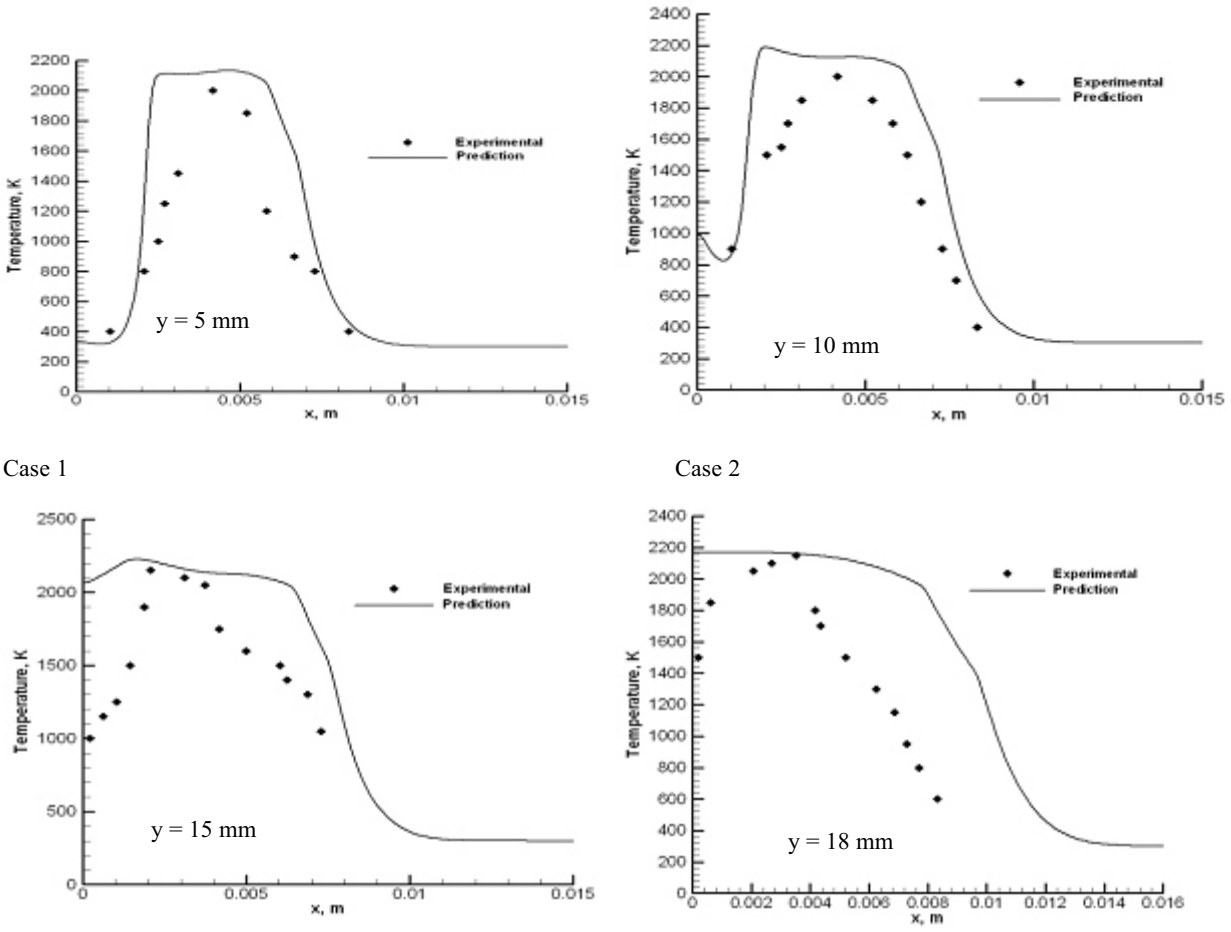

Case 1 Case 2

Case 3 Case 4

Fig. 5: Profiles of temperature at different positions above the burner

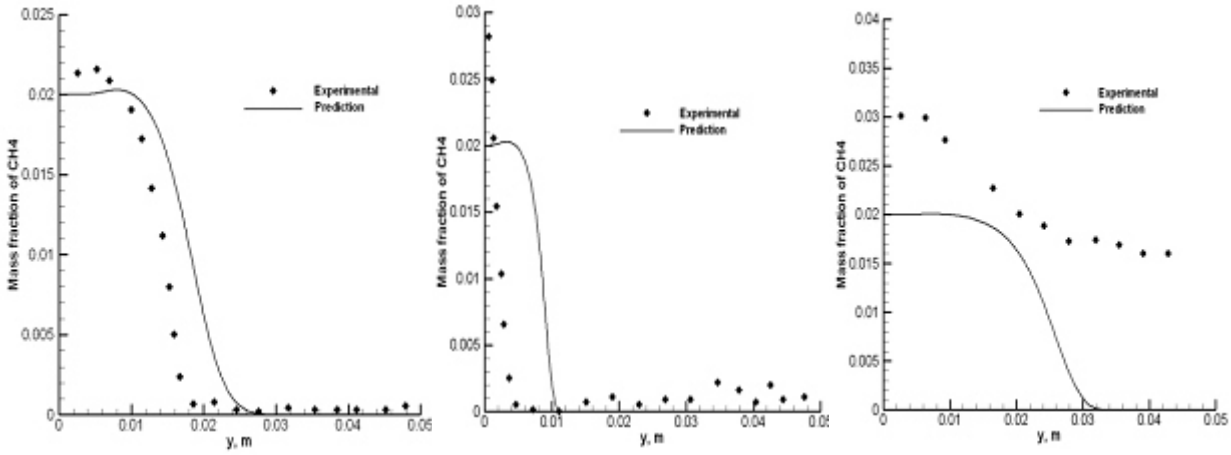

X = 0 mm X = 6 mm X = 10 mm

Fig. 6: Profiles of methane in the streamwise direction

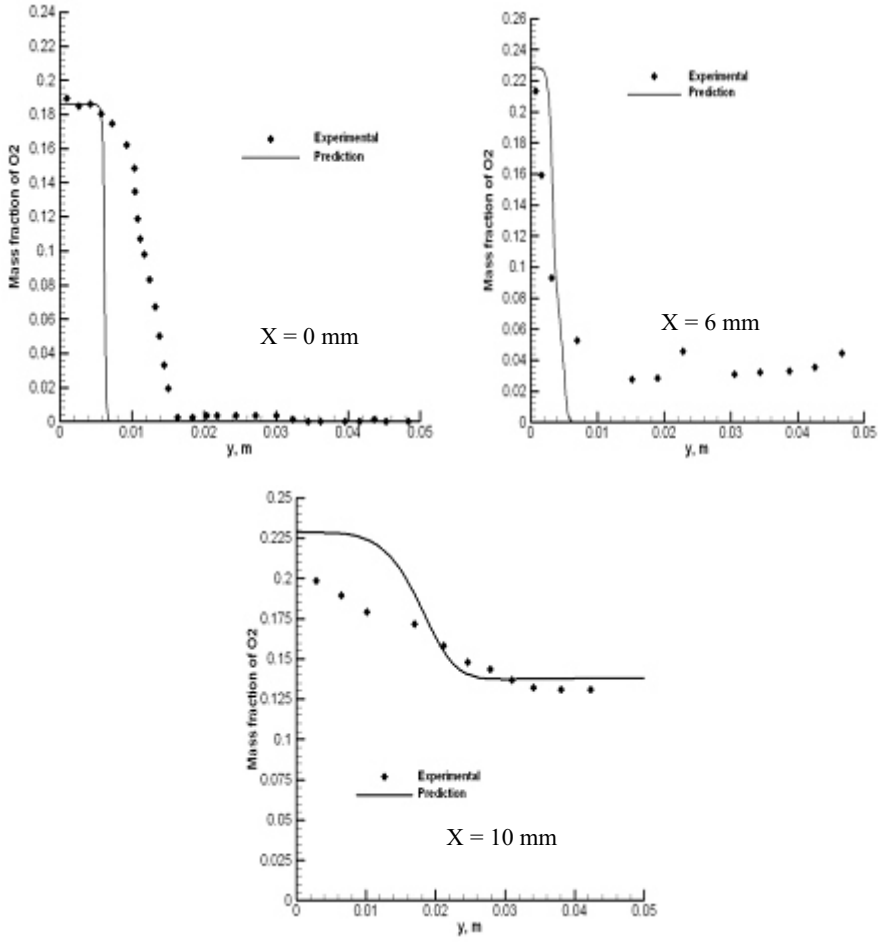

Fig. 7: Profiles of oxygen in the streamwise direction

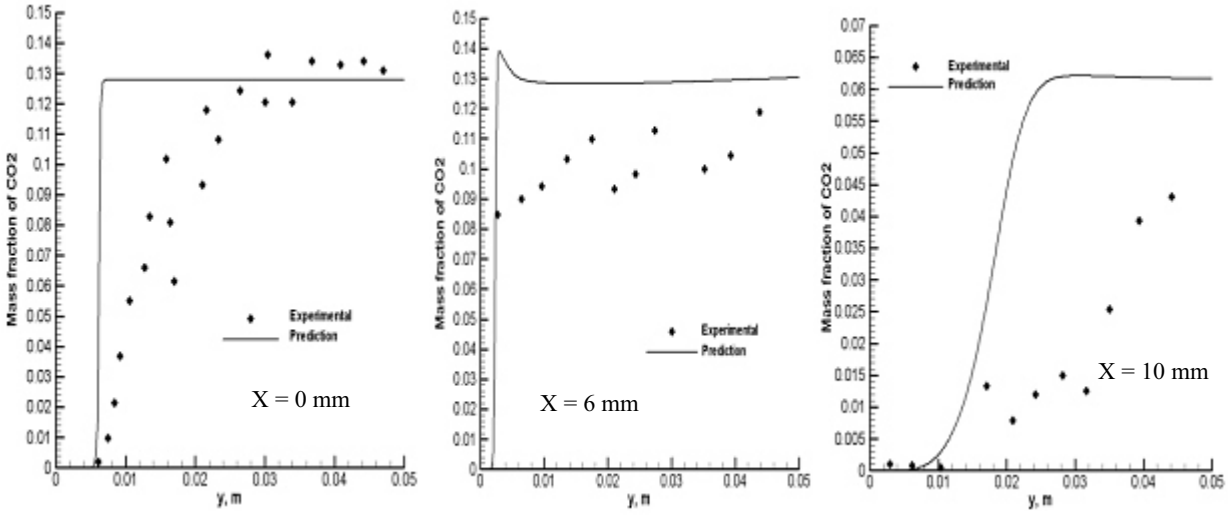

Fig. 8: Profiles of carbone dioxide in the streamwise direction

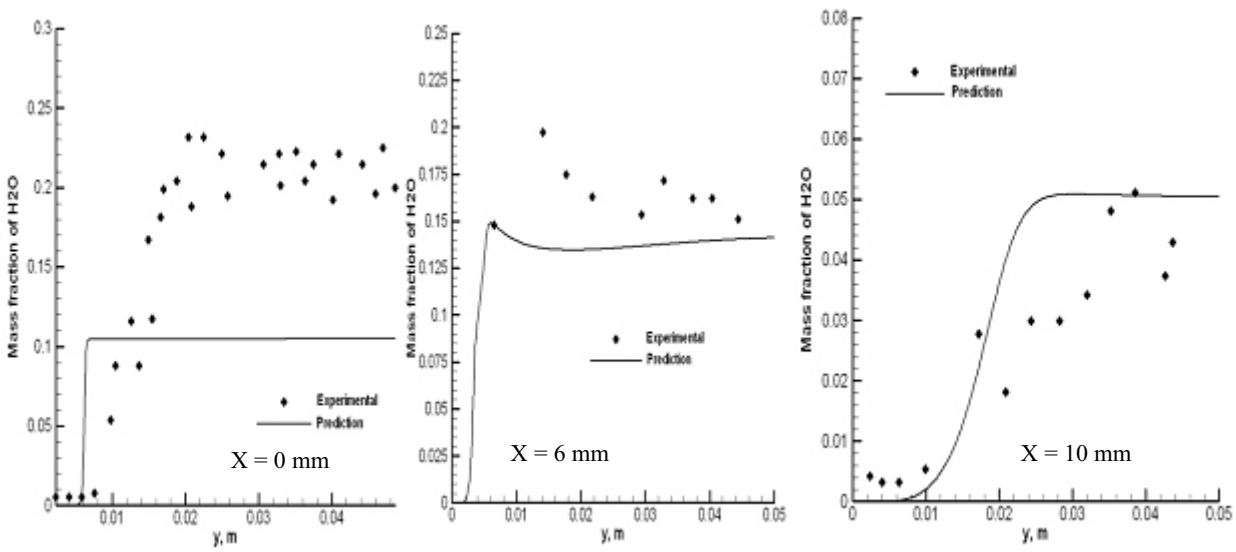

Fig. 9: Profiles of water in the streamwise direction

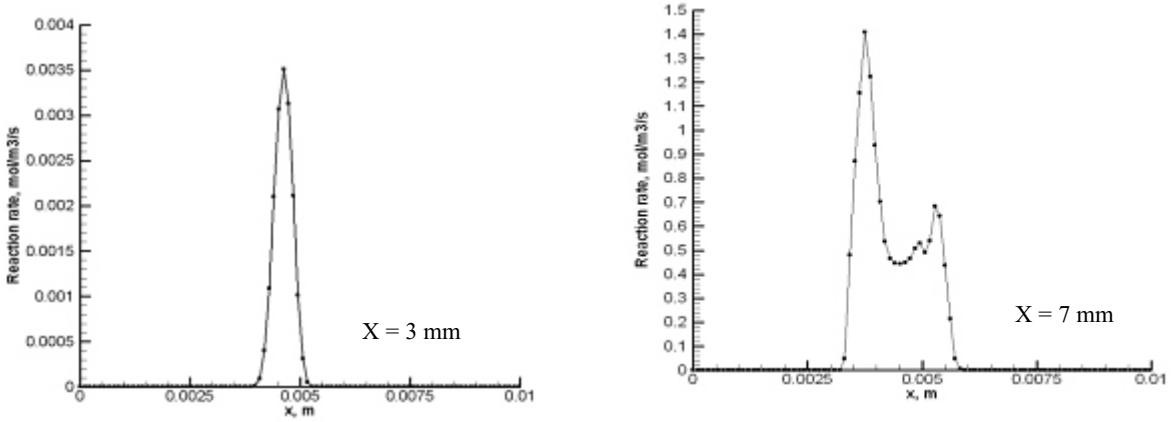

Case 1 Case 2

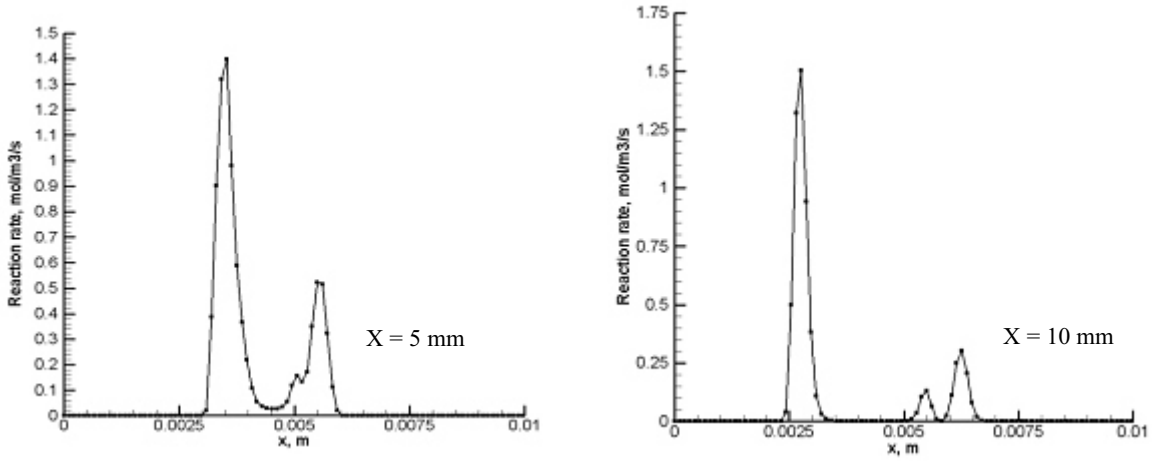

Case 3 Case 4

Fig. 10: Reaction rate for different position above the burner

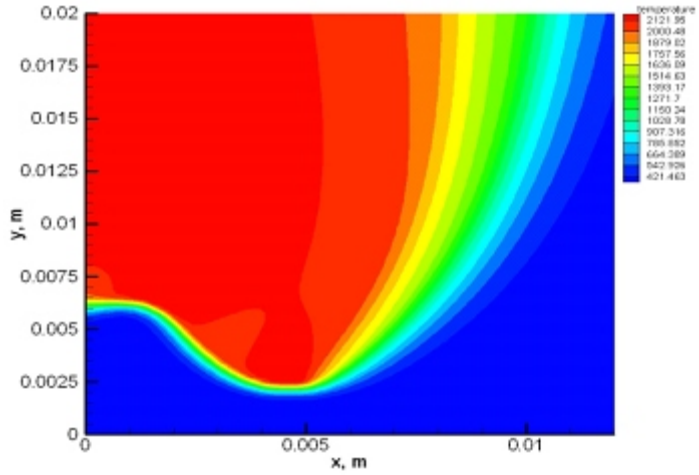

(I) Y_{CH_4} = 0.09

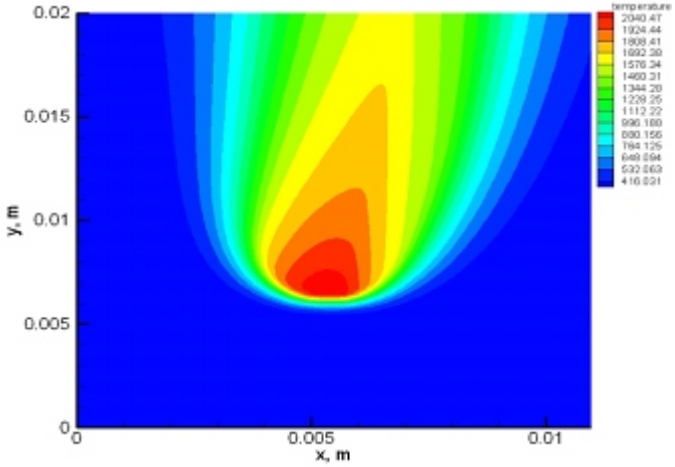

(II) Y_{CH_4} = 0.45

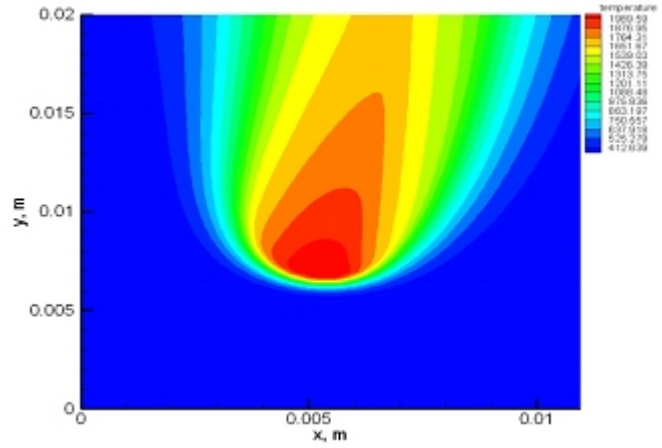

(III) Y_{CH_4} = 0.6

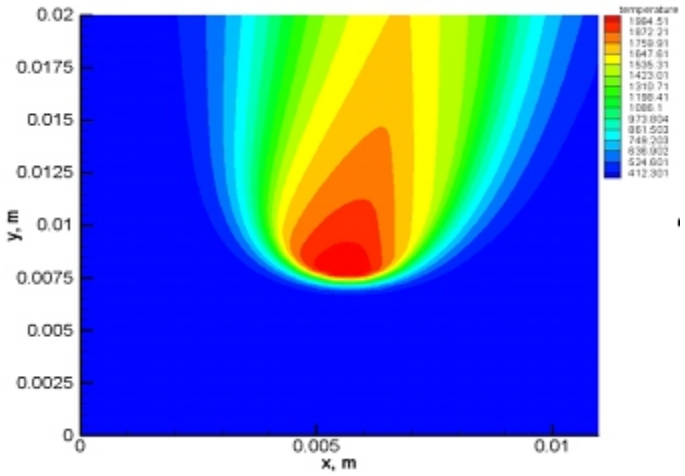

(IV) Y_{CH_4} = 0.8

Fig. 11: Contour of temperature of flame for different equivalence value ratio at 20 mm above the burner (in K)

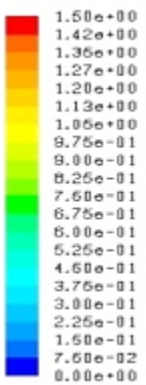

(I) Y_{CH_4} = 0.09

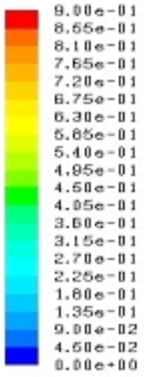

(II) Y_{CH_4} = 0.45

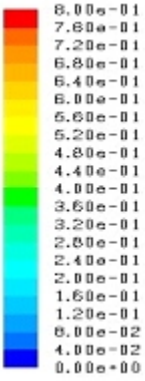

(III) Y_{CH_4} = 0.6

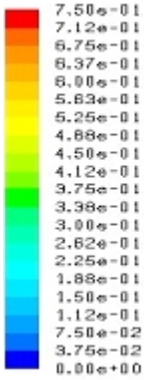

(IV) Y_{CH_4} = 0.8

Fig. 12: Contours of reaction rate (in unit of mol/m^3/s)

Table 3: Boundary conditions at the inlet of the duct for different cases

Case	(I)	(II)	(III)	(IV)
Velocity (m/s)	0.3	0.3	0.3	0.3
Temperature (K)	300	300	300	300
Fuel mass fraction (Y_{CH_4})	0.09	0.45	0.6	0.8
ϕ_{out}	0.35	0.35	0.35	0.35

Contours of temperature (in unit of K)

stoichiometric conditions between oxidizer and fuel which are conditions of maximal chemical reactivity. We can also deduce the increase of flame liftoff with the increase of inner equivalence ratios.

contours of reaction rate (Fig. 12) allow us to distinguish the three wings of triple flamme (rich premixed flame at the left, lean premixed flame at the right and the nonpremixed flame formed between the two premixed flames). The three wings merge at "triple point".

Contours of reaction rate and profiles of mass fraction of species enable us to report the decrease of the width of flame with the increase of inner equivalence ratio. We may explain this increase by the fact that in the presence of lean mixture (low fuel mass fraction in mixture), a rich mixture burns better for relatively small inner equivalence ratio as it remains around the stoichiometric conditions. Fig. 13 presents the consumption of reactants (fuel and oxidizer) and a simultaneous formation of products (CO_2 and H_2O). As we deal with lean and rich premixed combustion, there are respectively a rest of fuel in rich side and a rest of oxidizer in lean side which burn after diffusion process and produce the diffusion flame between the two premixed flames.

Profiles of reaction rate and their contours present the three wings of the "triple flame" (lean premixed flame, non premixed flame and the rich premixed flame) (Fig. 14).

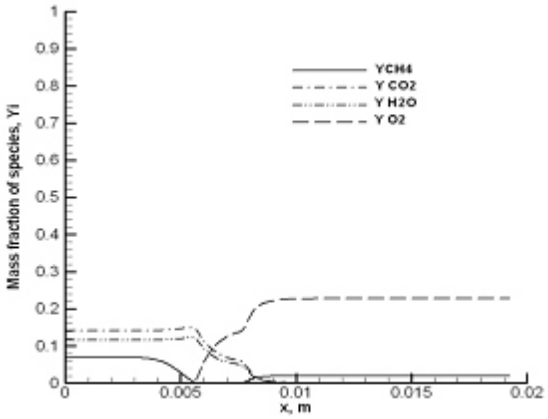

(I) Y_{CH_4} = 0.09

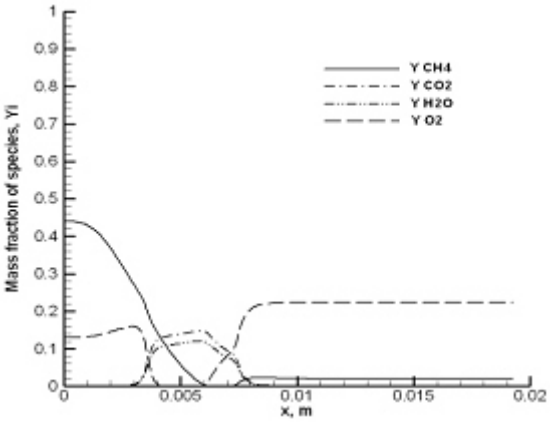

(II) Y_{CH_4} = 0.45

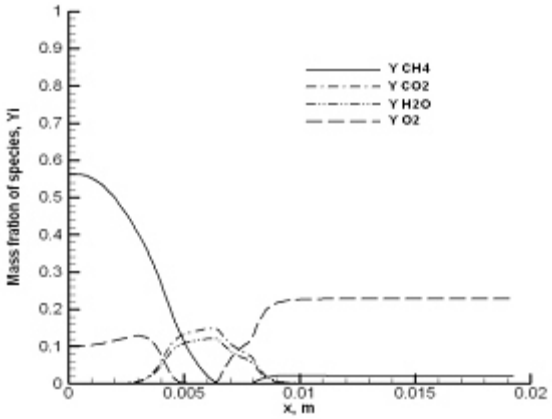

(III) Y_{CH_4} = 0.6

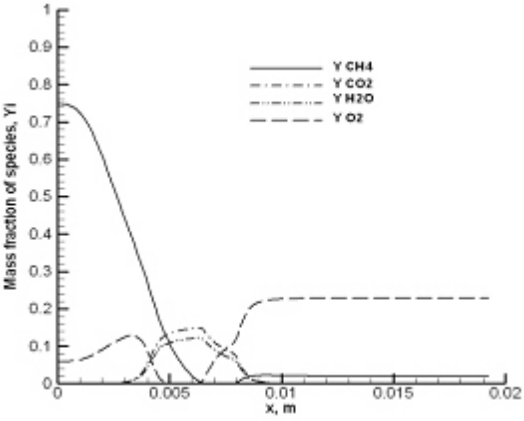

(IV) Y_{CH_4} = 0.8

Fig. 13: Profiles of mass fraction of species for different equivalence ratios

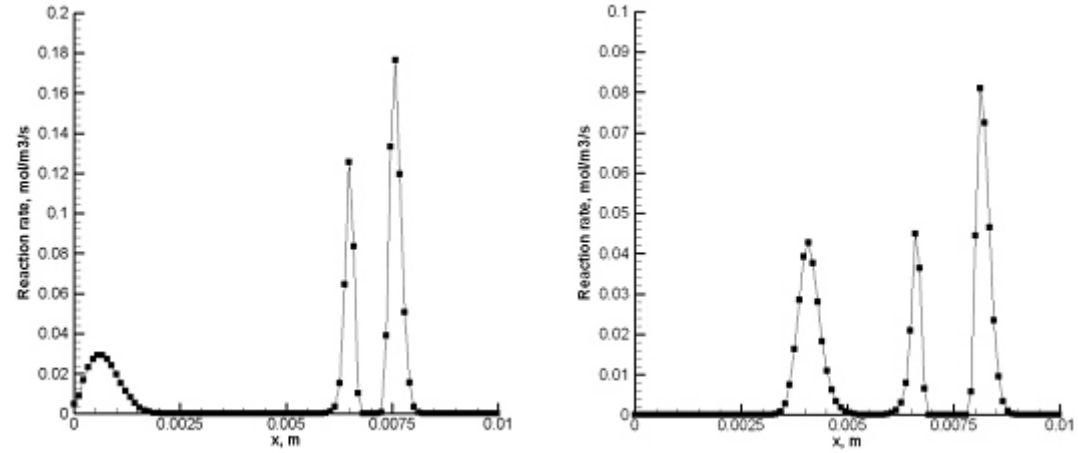

(I) Y_{CH_4} = 0.09 (II) Y_{CH_4} = 0.45

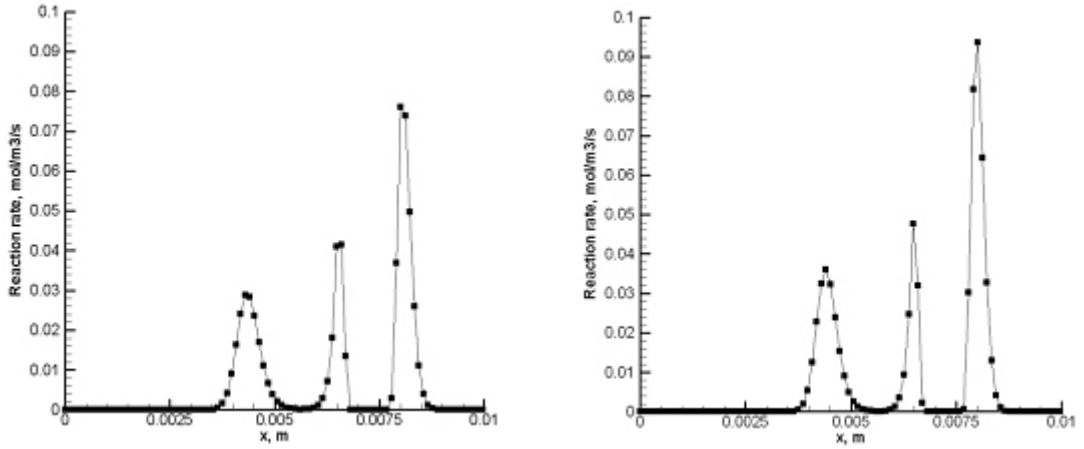

(III) Y_{CH_4} = 0.6 (IV) Y_{CH_4} = 0.8

Fig. 14: Profile of reaction rate at 15 mm above the burner (in unit of mol/m^3/s)

CONCLUSION

We have numerically investigated the structure of steady laminar two dimensional triple flames in order to contribute to the understanding of its structure. We have validated our numerical approach by comparing the computational and the experimental results. Secondly we have numerically studied the effect of equivalence ratio on the triple flame's structure by using the same approach.

- For the first part of our study, we can report a good prediction for a greater proportion of the species. Predicted temperatures and flames liftoff are in good agreement with experimental results, but some imperfections which may be related to our combustion model still remain (underestimation of some species and temperature). In order to solve the problem, we intend in future work to implement a new combustion model based on full detail chemistry in our CFD package; this assumption with the integration of ignition delay will enable us to better compute the rate of reaction and consequently the source term in the species' equation and finally the best values of mass fraction of species will be generated.
- In the second part, the behavior of the triple flames' structure during the increase of inner equivalence ratio suggest the decrease of triple flames' width, the increase of flames' liftoff and the decrease of maximum temperature. This numerical investigation may produce some new information on the triples' flames structure by integrating ignition delay in our new combustion model.

ACKNOWLEDGMENT

The authors express their gratitude to University Institute of Technology, University of Ngaoundéré for providing computer with license key of FLUENT code (FLUENT, 6.3.26).

NOMENCLATURE

Symbol	Physical Magnitude	Unity
C_{pk}	Specific heat at constant pressure of species i	J/Kg/K
C_{pm}	Mean Specific heat at constant pressure	J/Kg/K
D	Molecular diffusion coefficient	m^2/s
E	Activation energy	J/mol
h	Specific enthalpy of mixture	J/Kg
h_k	Specific enthalpy of species k	J/Kg
p	Pressure	N/m
ω_k	Reaction rate	$Mol/m^3/s$
R	Universal gas constant	J/mol/K
T	Temperature	K
U_i	i-directional velocity	m/s
W_k	Molecular weight of species k	Kg/mol
x	Lateral coordinate	m
y	Streamwise coordinate	m
ρ	Density	Kg/m^3
ϕ	Equivalence ratios	dimensionless

REFERENCES

Dold, J.W., 1989. Flame propagation in a nonuniform mixture: Analysis of a slowly varying triple flame. Combust. Flame, 76: 71-78.

FLUENT 6.3.26, UDF User Manual, Retrieved from: http://www.ANSYS.com.

FLUENT 6.3.26, User Manual, Retrieved from: http://www.ANSYS.com.

Kioni, P.N., B. Rogg, K.N.C. Bray and A. Linan, 1993. Flame spread in laminar mixing layers: The triple flame. Combust. Flame, 95: 276-290.

Muniz, L. and M.G. Mungal, 1997. Instantaneous flame-stabilisation velocities in lifted-. jet diffusion flames. Combust. Flame, 111: 13.

Noda, S. and S. Yamamoto, 2006. Identification of triple flame based on numerical data for laminar lifted flames. JSME Int. J. Ser. B, 49(3).

Obounou, M., M. Gonzalez and R. Borghi, 1994. A Lagrangian Models for Predicting Turbulent Diffusion Flames with Chemical Kinetic Effects. Combust. Inst., 25: 1107-1113.

Onuma, Y., T. Yamauchi, M. Mawatari, M. Morikawa and S. Noda, 2001. Low NOx combustion by a cyclone-jet combustor, JSME Int. J., Ser. B, 44(2): 559-574.

Phillips, H., 1965. In tenth Symposium (International) on Combustion. Cambridge, pp: 1277.

Puri, I.K., S.K. Aggarwal, S. Ratti and R. Azzoni, 2001. On the similitude between lifted and burner-stabilized triples flames: A numerical and experimental investigation. Combust. Flame, 124: 311-325.

Owston, R. and J. Abraham, 2010. Structure of hydrogen triple flames and premixed flames compared. Combust. Flame, 1: 14.

Ruetsch, G.R., L. Vervisch and A. Liman, 1995. Effect of heat release on triple flame. Phys. Fluids, 7: 1447.

Schefer, R.W. and P.J. Goix, Mechanism of flame stabilization in turbulent, lifted-jet flames. Combust. Flame, 112: 559-574.

Westbrook, C.K. and F.L. Dryer, 1981. Simplified Reaction Mechanisms for the oxidation of hydrocarbon fuels in flames. Combust. Sci. Technol., 27: 31-44.